Treatment of Pancreatic Cancer With an Oncolytic Adenovirus Expressing Interleukin-12 in Syrian Hamsters

Sergia Bortolanza[1], Maria Bunuales[1], Itziar Otano[1], Gloria Gonzalez-Aseguinolaza[1], Carlos Ortiz-de-Solorzano[2], Daniel Perez[2], Jesus Prieto[1,3] and Ruben Hernandez-Alcoceba[1]

[1]Division of Hepatology and Gene Therapy, University of Navarra, Pamplona, Spain; [2]Morphology and Imaging Unit, Center for Applied Medical Research (CIMA), University of Navarra, Pamplona, Spain; [3]CIBERehd, University Clinic, University of Navarra, Pamplona, Spain

Pancreatic cancer is an aggressive malignancy resistant to most conventional and experimental therapies, including conditionally replicative adenoviruses (CRAds). The incorporation of immunostimulatory genes such as interleukin-12 (IL-12) in these viruses may overcome some of their limitations, but evaluation of such vectors requires suitable preclinical models. We describe a CRAd in which replication is dependent on hypoxia-inducible factor (HIF) activity and alterations of the pRB pathway in cancer cells. Transgenes (luciferase or IL-12) were incorporated into E3 region of the virus using a selective 6.7K/gp19K deletion. A novel permissive model of pancreatic cancer developed in immunocompetent Syrian hamsters was used for *in vivo* analysis. We show that, in contrast with nonreplicating adenoviruses (NR-Ad), active viral production and enhanced transgene expression took place *in vivo*. A single intratumor inoculation of the CRAd expressing IL-12 (Ad-DHscIL12) achieved a potent antitumor effect, whereas higher doses of replication-competent adenoviruses carrying luciferase did not. Compared to a standard NR-Ad expressing IL-12, Ad-DHscIL12 was less toxic in hamsters, with more selective tumor expression and shorter systemic exposure to the cytokine. We conclude that the expression of IL-12 in the context of a hypoxia-inducible oncolytic adenovirus is effective against pancreatic cancer in a relevant animal model.

Received 29 July 2008; accepted 9 January 2009; published online 17 February 2009. doi:10.1038/mt.2009.9

INTRODUCTION

New treatment options are needed for devastating malignancies such as pancreatic cancer. Virotherapy is one of these alternatives, but clinical benefit has not been clearly demonstrated to date.[1] A variety of oncolytic adenoviruses (also called conditionally replicative adenoviruses, CRAds) has been designed following different strategies.[2] For controlling the expression of early viral genes, the use of promoters that are activated in a broad spectrum of tumors is an interesting option. Most solid tumors contain areas of low oxygen tension (hypoxia) due to the aberrant vasculature and uncoupled oxygen demand of rapidly growing tissues.[3] Under these circumstances, members of the hypoxia-inducible factor (HIF) family of transcription factors are stabilized and bind to a conserved sequence called hypoxia response element (HRE) found in the promoter of a variety of genes.[4] Natural or artificial promoters containing HREs have been used for the regulation of E1A in the construction of CRAds.[5–7] These viruses have demonstrated potent activation of their oncolytic effect in response to hypoxia and a remarkable antitumor effect on solid tumors. Activation of replication by HIF is a desirable characteristic of oncolytic agents because hypoxia is frequently associated with rapid progression and poor response to conventional therapies. Pancreatic cancer is a good example in which the strong activation of HIF pathways have been found to trigger downstream oncogenic routes.[8,9] Interestingly, the accumulation of HIF is an intrinsic characteristic of some cancer cells as part of the transformation process;[10] therefore, it is not always limited to hypoxic areas of the tumor. Finally, it has been described that tumor hypoxia attenuates replication of wild-type adenovirus, raising the possibility that this is limiting the potency of standard oncolytic adenoviruses.[11] Another common characteristic of cancer cells is the abrogation of pRB pathways that result in defects in the G1-S-phase checkpoint. Different genetic alterations found in tumors (mutations or deletions in tumor suppressor genes such as p16 and pRB, among others) converge in a phenotype characterized by accumulation of free transcription factors from the E2F family.[12] Therefore, regulatory sequences that respond to E2Fs (including the E2F-1 promoter itself)[13] have been proposed as wide-range promoters for transcriptional control of viral replication.[6,14,15] In addition, the 922-947 deletion of E1A viral gene (affecting the CR2 domain responsible for binding to pRB) prevents E1A sequestration of pRB and subsequent elevation of free E2Fs in quiescent cells infected by the virus. This deletion preserves full potency of the virus in cancer cells while causing attenuation in quiescent cells.[16,17] Oncolytic adenoviruses that include E1A CR2 deletions alone,[16,17] or in combination with the E2F-1 promoter regulating E1A and E4 viral regions,[18,19] have demonstrated increased cancer specificity and potent antitumor effects in different animal models. In addition, much effort is now focused on arming CRAds with therapeutic genes that will avoid the need of extensive virus spread. An attractive strategy is the use of immunostimulatory cytokines

Correspondence: *Ruben Hernandez-Alcoceba, Edificio CIMA, Av. Pio XII, 55, 31008-Pamplona, Navarra, Spain. E-mail: rubenh@unav.es*

such as interleukin-12 (IL-12). This heterodimeric protein composed of p35 and p40 subunits possess multiple effects on different cell populations, acting as a bridge between innate and adaptive immune responses.[20] Replication-deficient adenoviral vectors expressing IL-12 have shown promising results on different tumor models.[21–23] An adequate evaluation of antitumor effect and toxicity of CRAds carrying immunostimulatory genes has been impaired by the lack of immunocompetent animal models in which adenovirus can replicate. We and others have recently demonstrated that the Syrian hamster is a suitable host in which different tumors permissive for adenoviral replication can be developed.[24,25] In the present work, we have combined different regulatory mechanisms for the development of an optimized CRAd expressing IL-12 and describe its antitumor activity, which makes this vector a promising option for inoperable pancreatic cancer in humans.

RESULTS

New HIF-dependent CRAds adapted as gene therapy vectors retain their responsiveness to hypoxia

The new CRAds include the following features: (i) control of E1A and E4 transcription units with an hypoxia-responsive promoter and E2F-1 promoters, respectively; (ii) partial deletion of E1A (CR2 domain for pRB binding); and (iii) deletion of the 6.7K/gp19K genes in the E3 region in order to accommodate foreign genes.[26] Based on the structure of the previously reported HIF-inducible virus, we have introduced a 922-947 deletion in the E1A gene to avoid interaction with Rb in normal cells and have inserted exogenous genes (the reporter luciferase gene or the immunostimulatory cytokine IL-12) in the E3 region, thus generating, respectively, Ad-DHLuc and Ad-DHscIL12 vectors (**Figure 1a**). In order to study the influence of the partial E1A deletion on the performance of the vectors, we constructed the Ad-HLuc virus, in which wild-type E1A gene is maintained. As a control, we constructed a nonregulated wild-type adenovirus carrying luciferase in the same genomic location (Ad-WTLuc). In order to verify that the new CRAds retain the responsiveness to HIF, we infected human cell lines HuH-7 (hepatocellular carcinoma), A549 (squamous cell carcinoma), and IMR-90 (normal fibroblasts) with Ad-HLuc, Ad-DHLuc, or wild-type adenovirus type 5 (Ad-WT). Cells were maintained under standard culture conditions (normoxia, atmospheric air) or hypoxia (1% oxygen), and 48 hours later, cells were collected and the production of the late viral protein fiber was analyzed by western blot (**Figure 1b**). Because expression of fiber takes place only after viral replication has been activated, it serves as an indicator of different regulatory systems working together in the virus. As expected, fiber expression was increased in CRAd-infected cells growing under hypoxic conditions, whereas Ad-WT was unaffected. In normoxia, fiber expression was higher for Ad-HLuc than Ad-DHLuc in all cell lines. More important, fiber expression in normal cells (IMR-90) infected with Ad-DHLuc is very low even under hypoxic conditions, suggesting a strong attenuation of this virus in nontumor cells. These data show that the deletion introduced in E1A efficiently hampered vector replication in normal cells. In order to verify activation of the hypoxia program in our assay conditions, we confirmed that all the cells experienced accumulation of HIF-1α when they were maintained at low oxygen tension (**Figure 1c**), including the Syrian hamster pancreatic

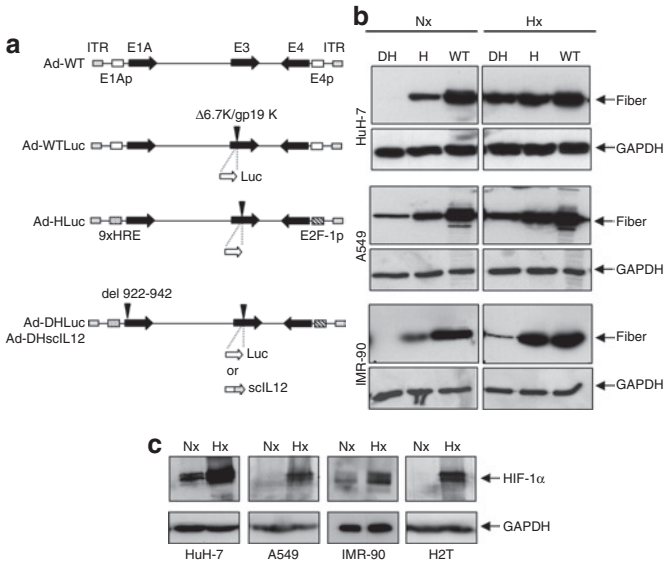

Figure 1 Influence of hypoxia on the activity of hypoxia-inducible factor (HIF)-dependent conditionally replicative adenoviruses. (**a**) Schematic representation of the genomes of replication-competent adenoviruses used in this study. (**b**) Western blot of fiber in human cancer (HuH-7 and A549) and normal (IMR-90) cells infected with Ad-DHLuc (DH), Ad-HLuc (H), and Ad-WT (WT). Infection was carried out for 2 hours at MOI 10 and 100 for cancer and normal cells, respectively. Cells were then washed and incubated with fresh culture medium in normoxic (Nx) or hypoxic condition (1% O_2, Hx). Cell extracts were obtained 2 days later. (**c**) Western blot of HIF-1α in human HuH-7, A549, IMR-90, and hamster H2T cells maintained under normoxic or hypoxic conditions during 12 hours. Glyceraldehyde-3-phosphate dehydrogenase is shown to verify homogeneous loading of samples.

cancer cells H2T, which will be used further *in vitro* and *in vivo* studies. We also analyzed the specificity of the viruses in their ability to destroy cell lines according to the basal activity of the HIF pathway. We used RCC10 cells that are derived from a human renal cell carcinoma that presents a constitutive elevation in HIF-1α due to the lack of a functional VHL protein. As a control, we employed the VHL53 clone, where VHL is restored through stable transfection of the correct VHL gene; therefore, basal levels of HIF-1α are drastically reduced.[5] We infected these cells with Ad-DHLuc, Ad-HLuc, Ad-WT, and the previously described Ad9xHRE1A virus. As shown in **Figure 2a**, all hypoxia-regulated viruses were active in RCC10 cells but attenuated in VHL53, whereas Ad-WT caused the same degree of cell destruction irrespective of the VHL status of the cells. Taking into account that survival was quantified 1 week after infection, the marked reduction in the viability of the cultures depends on viral amplification.

Viral replication and cytolysis mediated by Ad-DHLuc are repressed in normal cells without reducing its oncolytic capacity

In order to evaluate the impact of the E1A CR2 deletion on the tumor specificity of the virus, we compared Ad-DHLuc and Ad-HLuc in terms of cytolytic potency and replication on normal and cancer cells. In **Figure 2b** we represent the percentage of HuH-7 cells that survive 5 days after infection with different MOIs under hypoxic or normoxic conditions. As expected, the cytopathic effect caused by both viruses was equally stimulated by

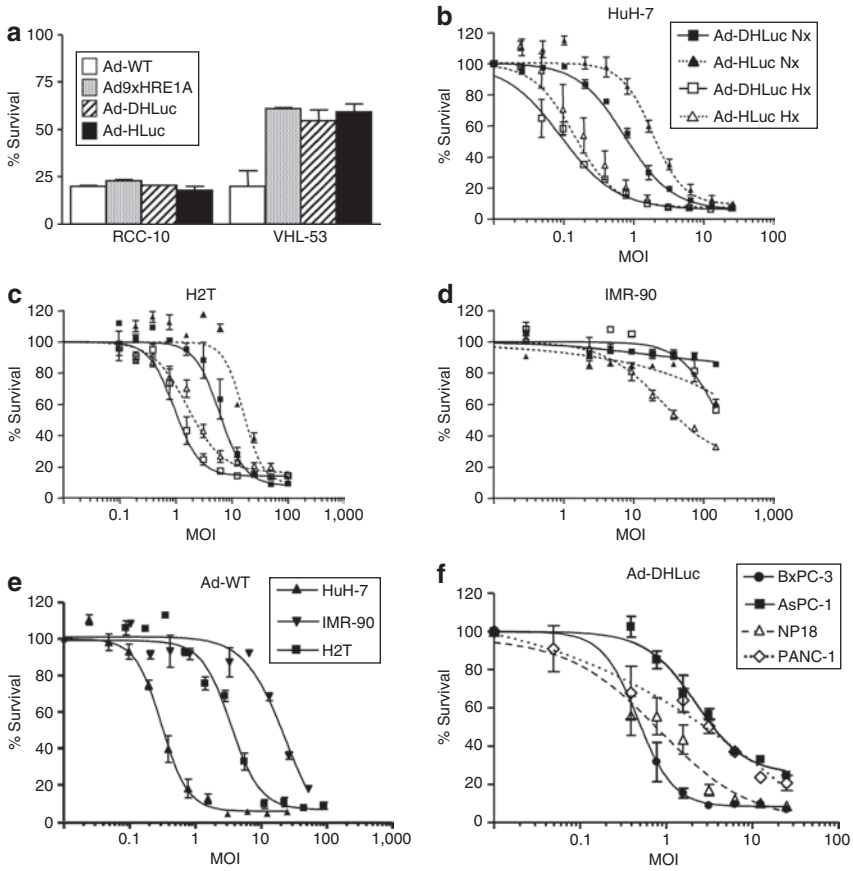

Figure 2 Cytolytic effect of viruses. (**a**) Cells with normal or constitutively activated HIF pathways (VHL53 and RCC-10, respectively) were infected with Ad-DHLuc, Ad-HLuc, Ad-WT, or Ad9xHRE1A viruses and maintained for 7 days under normoxic conditions until viability was determined. The percentage of surviving cells versus noninfected controls is represented. (**b–d**) Influence of the E1A CR2 deletion. (**b**) HuH-7, (**c**) H2T, and (**d**) IMR90 cells were infected with Ad-DHLuc or Ad-HLuc at the indicated MOIs and cultured under normoxia (Nx, black symbols) or hypoxia (Hx, white symbols) for 5 (HuH-7, H2T) or 9 days (IMR-90). (**e**) Cytolytic effect of the Ad-WT on HuH-7, H2T, and IMR-90 cells under normoxic conditions. (**f**) Cytolytic effect of Ad-DHLuc on human pancreatic cancer cell lines BxPC-3, AsPC-1, NP18, and PANC-1 under normoxic conditions. Viability was determined 5 days after infection in **e** and **f** panels. The percentage of surviving cells versus noninfected controls is represented as a sigmoidal dose–response curve. Each curve is a representative experiment from at least four performed in triplicate.

hypoxia on this cancer cell line. The same was observed in the H2T cells (**Figure 2c**), demonstrating the functionality of the system in Syrian hamster cells. When the same experiment was performed on IMR-90 cells (**Figure 2d**), Ad-HLuc was activated by hypoxia in a wide range of MOIs, as observed in cancer cell lines. In contrast, significant activation of Ad-DHLuc only took place at the highest MOI of 150, indicating a deeper attenuation of the virus. In **Figure 2e** we show the viability of Huh-7, H2T, and IMR-90 cells exposed to Ad-WT under normoxic conditions. No significant changes were observed in hypoxia (data not shown). Together, these results indicate that Ad-DHLuc can reach a cytolytic effect close to Ad-WT on cancer cells when it is activated by hypoxia; however, it remains attenuated in normal cells. Finally, we verified that human pancreatic cell lines PANC-1, AsPC-1, BxPC-3, and NP18 can be efficiently eliminated by Ad-DHLuc under hypoxic conditions (**Figure 2f**). The higher susceptibility of BxPC-3 and NP18 cells correlates with higher infectivity. The same trend was observed in terms of virus replication (data not shown).

The modulation of viral replication was confirmed in the virus burst-size determination shown in **Figure 3**. In this experiment, we observed that the amount of infective particles generated in a

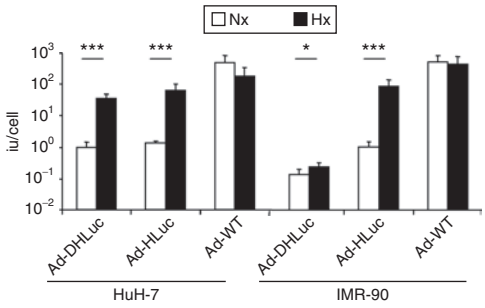

Figure 3 Stimulation of viral replication by hypoxia in normal and tumor cells. Cells were infected for 2 hours with Ad-DHLuc, Ad-Hluc, and Ad-WT at MOI 10 (HuH-7) or 100 (IMR-90). Then virus was removed and cells were washed and maintained in normoxia (Nx) or hypoxia (Hx) for 48 hours. The amount of infective virus extracted from cell lysates is represented as iu/cell. $*P < 0.05$, $***P < 0.0001$.

single viral cycle is greatly stimulated by hypoxia in HuH-7 cells infected with Ad-HLuc and Ad-DHLuc. In contrast, this increase in viral progeny production was attenuated in IMR-90 cells infected with Ad-DHLuc compared with the robust (100-fold) activation of Ad-HLuc. Ad-WT showed no variation or a slight

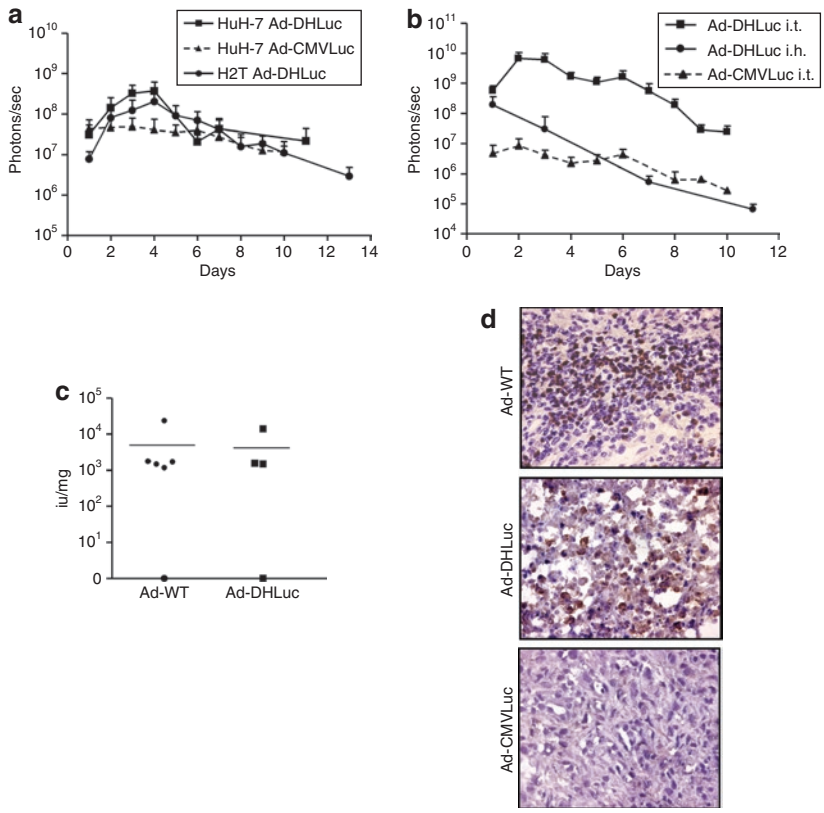

Figure 4 Transgene expression and replication of Ad-DHLuc *in vivo*. (**a**) Tumor xenografts were induced in the flank of *nu/nu* mice by subcutaneous inoculation of HuH-7 or H2T cells. When tumors reached at least 150 mm^3 volume, a single dose of 2×10^8 iu Ad-DHLuc was injected intratumorally. The same dose of Ad-CMVLuc was injected in HuH-7 xenografts for comparison. Luciferase activity was analyzed over time and quantified (in photons/s) using an *in vivo* bioluminescence detection system. (**b**) Liver metastases of pancreatic cancer were established in Syrian hamsters by intrahepatic injection of H2T cells. One month later, 2×10^9 iu of Ad-DHLuc (squares), or Ad-CMVLuc (triangles, dotted line) were injected intratumorally ($n = 5$). In a separate group, healthy hamsters were inoculated intrahepatically with Ad-DHLuc (circles). Luciferase activity was measured daily. (**c**,**d**) Pancreatic tumors were obtained as indicated for panel **b**. Ad-DHLuc or Ad-WT were inoculated intratumorally at 2×10^9 iu/hamster. Four days later, animals were sacrificed and each tumor was divided in two. One half was lyzed for determination of viable viral particles and is represented as iu/mg tumor for each animal (**c**). The other portion was processed for detection of adenoviral capsid proteins in frozen sections as indicated (**d**). Positive cells display brown staining. A section from a tumor inoculated with the same dose of Ad-CMVLuc is included as a negative control for replication. Representative pictures at ×400 magnification are shown.

decrease in replication in response to hypoxia. The same result was obtained with the Ad-WTLuc virus (data not shown).

Ad-DHLuc replicates and amplifies transgene expression *in vivo*

The performance of Ad-DHLuc as a gene therapy vector *in vivo* was compared with a nonreplicating adenoviruses (NR-Ad) expressing luciferase under the control of the CMV promoter (Ad-CMVLuc). We started with a standard xenograft model induced by subcutaneous inoculation of cancer cells in athymic mice. This allowed us to compare the kinetics and biodistribution of Ad-DHLuc in tumors derived from HuH-7 and H2T cells in the same conditions. The virus was administered intratumorally as a single injection of 2×10^8 iu, and luciferase expression was monitored by bioluminescence detection. Photon emission was confined to the tumor area during all the observation period (data not shown). In **Figure 4a** we represent the quantification of luciferase expression over time. HuH-7 tumors injected with Ad-DHLuc experienced a gradual increase in luciferase activity during the first 4 days after injection, reaching a tenfold increment, and then the activity declined. The same pattern was observed for H2T tumors, with a 20-fold increase at day 4. In contrast, luciferase signal in HuH-7 tumors injected with Ad-CMVLuc showed a slow decay from day 1, without a period of signal amplification. Next, we performed similar experiments in the Syrian hamster model. H2T cells were implanted in the liver, and viruses (2×10^9 iu) were administered by intratumor injection 1 month later. As illustrated in **Figure 4b**, a clear difference between both viruses was observed. Compared with Ad-CMVLuc, Ad-DHLuc showed higher luciferase expression (100-fold) starting from day 1, and a rapid increase with peak values at days 2–3. In contrast, when the same dose of Ad-DHLuc was injected in the liver of healthy hamsters, a rapid and continuous decline in bioluminiscence was observed, suggesting that the increase in luciferase expression comes mainly from the infected cells in the tumor and not the surrounding liver. Together, these data are compatible with active viral replication of Ad-DHLuc in tumors. However, no direct correlation between replication and luciferase activity *in vivo* can be assumed because amplification of the signal can be masked by the cytopathic effect and the immune reaction against infected cells. To directly demonstrate replication, animals bearing

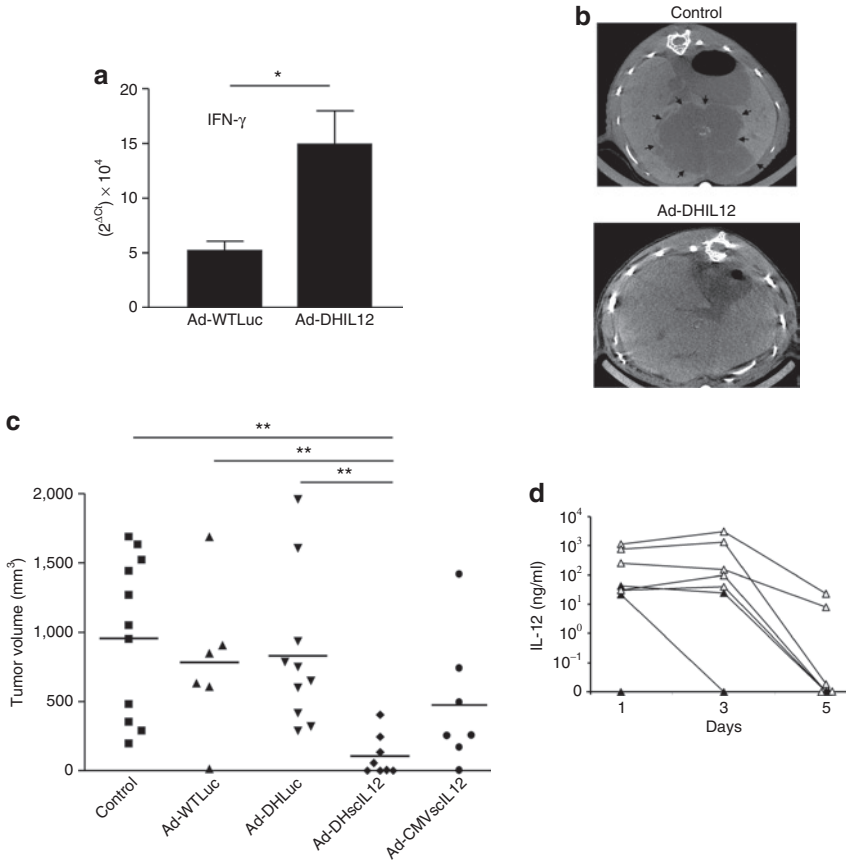

Figure 5 Biological activity and antitumor effect of Ad-DHscIL12 in liver metastases of pancreatic cancer in hamsters. Liver metastases of pancreatic cancer were established in Syrian hamsters by intrahepatic injection of H2T cells. Five weeks later, tumors were inoculated with a single dose of Ad-DHscIL12 or Ad-DHLuc at 2×10^7 iu; Ad-WTLuc at 2×10^9 iu, Ad-CMVscIL12 at 10^7 iu, or saline solution. (**a**) Some animals ($n = 4$) treated with Ad-WTLuc or Ad-DHscIL12 were sacrificed 3 days after vector administration, and expression of hamster interferon (IFN)-γ was analyzed by quantitative reverse transcriptase-PCR in tumor samples. (**b**) One month after virus inoculation, abdominal micro-CT was performed in hamsters treated with Ad-DHscIL12 or saline as indicated. Horizontal sections of representative animals are shown. Arrows indicate the margins of the tumor. (**c**) All animals were then sacrificed and tumor volume was directly measured at necropsy. (**d**) Serum was collected at days 1, 3, and 5 after virus injection, and murine interleukin (IL)-12 was determined by ELISA. White and black triangles represent animals that experienced complete or partial antitumor effect at the end of the experiment, respectively. *$P < 0.05$, ** $P < 0.01$.

intrahepatic H2T tumors were injected with Ad-DHLuc or Ad-WT and sacrificed 4 days later. Quantification of infective viruses was carried out in tissue homogenates from these tumors (**Figure 4c**). Viral progeny production was detected in all the tumors, except for one example in each group. To further demonstrate active viral replication, we performed immunohistochemistry of tumor sections for the detection of late viral proteins. In **Figure 4d** we show representative examples indicating areas of positively stained cells in the tumors infected with Ad-DHLuc and Ad-WT. In contrast, tumor sections from hamsters inoculated with Ad-CMVLuc were negative. Overall, the analysis of both parameters confirms that replication of Ad-DHLuc takes place with an efficacy comparable to Ad-WT in pancreatic tumors.

Ad-DHscIL12 inhibits the growth of pancreatic cancer in the liver of immunocompetent Syrian hamsters

Pancreatic tumors were induced by intrahepatic inoculation of H2T cells in hamsters.[25] The appearance of tumors was verified 5 weeks later by laparotomy, and 2×10^7 iu of Ad-DHscIL12 or Ad-DHLuc was inoculated intratumorally at this moment. Other animals received a standard NR-Ad vector expressing scIL-12 under the control of a CMV promoter (Ad-CMV-scIL12) at a lower dose (10^7 iu) in order to avoid severe toxicity (see the section, "Selective expression of IL-12 in tumors reduces the toxicity of Ad-DHscIL12"). A fourth group received Ad-WTLuc at high dose (2×10^9 iu) to determine whether some antitumor effect can be obtained by direct viral oncolysis in this model. Finally, other animals were injected with the same volume of saline solution as a negative control. To demonstrate the biological activity of the murine scIL-12 expressed by Ad-DHIL2 in hamsters, some animals were sacrificed 3 days after vector inoculation, and the expression of interferon (IFN)-γ was analyzed in tumor samples by real-time quantitative PCR. As shown in **Figure 5a**, specific stimulation of IFN-γ expression was observed in Ad-DHscIL12–treated animals as compared with those treated with a higher dose of Ad-WTLuc. This supports our *in vitro* data showing that murine IL-12 stimulates the production of IFN-γ in peripheral blood mononuclear cell derived from Syrian hamster (data not shown). In order to evaluate the antitumor effect without performing a new laparotomy, hamsters underwent abdominal

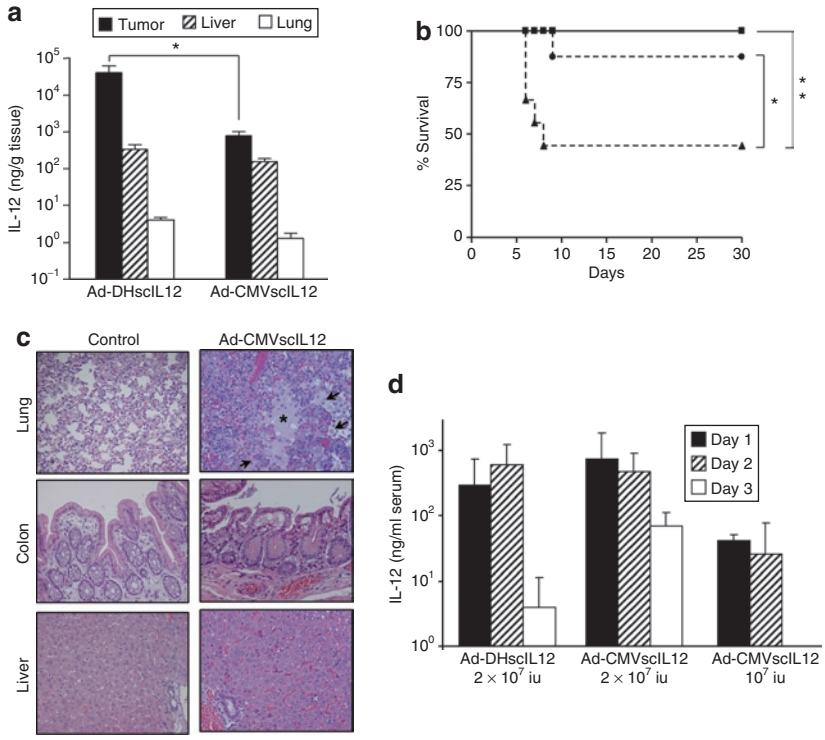

Figure 6 Specificity of interleukin (IL)-12 expression and toxicity of Ad-DHscIL12 and Ad-CMV-scIL12 viruses. Liver metastases of pancreatic cancer were established in Syrian hamsters by intrahepatic injection of H2T cells. Five weeks later, tumors were inoculated with a single dose of Ad-DHscIL12 at 2×10^7 iu (squares), or Ad-CMV-scIL12 at 2×10^7 iu (triangles) or 10^7 iu (circles). (**a**) One set of animals corresponding to the high-dose groups ($n = 5$) were sacrificed 3 days after virus inoculation for organ collection. The concentration of IL-12 was measured by ELISA in homogenates from tumors, livers, and lungs, as indicated. Values are expressed as ng IL-12/g tissue. (**b**) The rest of the animals ($n = 8$ in each group), were monitored for survival. *$P = 0.019$, **$P = 0.002$, log-rank test. (**c**) Histological analysis of lung, colon, and liver from a moribund hamster 6 days after treatment with 2×10^7 iu of Ad-CMV-scIL12, compared with a control animal inoculated with saline solution. Inflammatory infiltration and edema found in the lungs of the vector-treated hamster are marked by arrows and asterisk, respectively (Hematoxylin-Eosin staining of paraffin-embedded sections, ×200 magnification). (**d**) Concentration of IL-12 in serum determined at days 1, 3, and 5.

micro-CT 1 month after virus administration. We could detect reduction in tumor growth only in animals treated with Ad-DHscIL12. In Figure 5b, top panel, we show a representative example of a control animal (saline injection) in which extensive areas of tumor were evidenced infiltrating the liver parenchyma (arrows). In contrast, bottom panel illustrates a hamster that experienced a complete response to the treatment with Ad-DHscIL12, showing no major alterations in hepatic structure. All animals were then sacrificed and direct tumor measurement was performed. Tumor volumes of individual hamsters are represented in Figure 5c. The only group showing a significant reduction in tumor progression corresponded to Ad-DHscIL12. Four of the animals were completely tumor free, another one showed only residual disease, and the remaining two had a partial response. In order to investigate the relationship between antitumor effect and expression of the therapeutic gene, murine IL-12 was determined by ELISA in the serum of animals treated with Ad-DHscIL12 during the first week. As shown in Figure 5d, high variability was observed, probably due in part to differences in the efficacy of tumor inoculation. Maximum concentrations of approximately 10^3 ng/ml were observed during the first 3 days, followed by a sharp decline at day 5. Interestingly, animals with reduced antitumor response coincided with those with lower IL-12 expression (marked as black triangles in Figure 5d).

Selective expression of IL-12 in tumors reduces the toxicity of Ad-DHscIL12

We studied whether the controlled replication of Ad-DHscIL12 could restrict the production of IL-12 into the tumors and increase the safety of the virus, compared with the nonregulated vector Ad-CMV-scIL12. To this end, intrahepatic H2T tumors were treated with 2×10^7 iu of Ad-DHscIL12 or Ad-CMV-scIL12, and hamsters were sacrificed 3 days later for quantification of IL-12 content in different organs (Figure 6a). In agreement with results obtained with the reporter gene luciferase, Ad-DHscIL12 achieved higher IL-12 expression in the tumors compared with the nonreplicative vector (~50-fold difference in this case). In contrast, the concentration of IL-12 in normal liver was similar between both vectors. We observed no difference in expression between the liver surrounding the tumor and a distant hepatic lobe (data not shown), suggesting that infection of hepatocytes is due to the virus present in the bloodstream and not to local spreading from the inoculated tumor. In addition, no virus replication was detected in liver samples from these animals (data not shown). As expected, low expression of IL-12 was observed in the lung. Therefore, Ad-DHscIL12 shows preferential expression in the tumors and is able to minimize the effect of infection in nontarget organs. In order to directly compare toxicity of Ad-DHscIL12 and Ad-CMV-scIL12 vectors in these experimental conditions, survival and serum IL-12

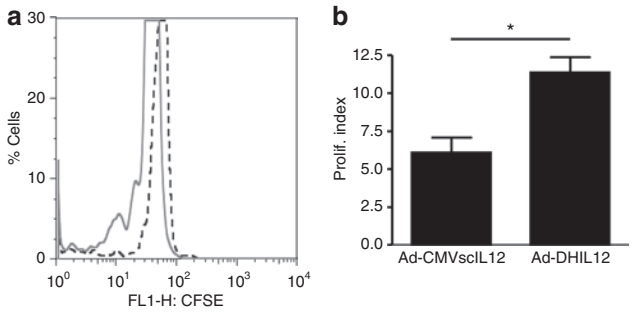

Figure 7 Ad-DHscIL12-treated hamsters develop H2T-specific immune responses. (**a**) Hamsters bearing H2T tumors were treated with Ad-DHscIL12 (continuous line) or Ad-CMV-scIL12 (dotted line). Twenty days later, peripheral blood mononuclear cell from these animals were labeled with CFSE and incubated with irradiated H2T cells for 3 days. Histogram displaying fluorescence intensity of leukocytes from one representative animal in each group is represented. (**b**) Average proliferation index of each group ($n = 3$). *$P < 0.05$.

concentrations were monitored in hamsters that received the same treatments described above. Intratumor administration of 2×10^7 iu Ad-CMV-scIL12 caused severe toxicity and death of >50% of hamsters in the first week after treatment (**Figure 6b**). Histopatological analysis of different organs revealed intense inflammatory infiltration and edema in lungs, whereas liver and colon showed no major alterations (**Figure 6c**). In contrast, the same dose of Ad-DHscIL12 was well tolerated, and all animals survived for >1 month. Severe toxicity of Ad-DHscIL12 appeared at 8×10^7 iu/hamster (data not shown), and the maximum tolerated dose for this vector is 4×10^7 in this model. A low dose of Ad-CMV-scIL12 (10^7 iu/hamster) was less toxic (**Figure 6b**), but only a discrete (no statistically significant, $P = 0.07$) reduction in tumor volume was observed (**Figure 5c**). In **Figure 6d** we show the concentration of IL-12 in the serum of these animals. As previously observed, hamsters treated with Ad-DHscIL12 showed a short course of IL-12 expression with peak concentration at day 3 and a rapid decline. In the case of Ad-CMV-scIL12, maximum serum concentration of IL-12 was observed at day 1, and was not significantly different from the previous group. However, IL-12 expression was more stable over time, which could account for the increased toxicity of this vector. Finally, Ad-CMV-scIL12 at 10^7 iu achieved very low levels of IL-12.

Ad-DHscIL12 stimulates the immune response against cancer cells

To verify the participation of the immune system on the antitumor effect of Ad-DHscIL12, peripheral blood mononuclear cell from treated animals were exposed to H2T tumor cells *in vitro*. Proliferation of leukocytes was assessed by carboxyfluorescein succinimidyl ester labeling and flow cytometry. As an example of noneffective treatment, the response was also studied in hamsters that received 10^7 iu of Ad-CMV-scIL12. Significant stimulation of proliferation was only observed in the Ad-DHscIL12 group (**Figure 7**), suggesting that activation of the immune response against cancer cells may explain in part the antitumor effect of this CRAd in our model.

DISCUSSION

In the present work, we have optimized a regulatory system based on the transcriptional control of E1A and E4 viral regions with HIF and E2F-1-dependant promoters, respectively, in combination with a partial deletion in the CR2 domain of E1A. These modifications achieve a robust control of viral replication and cytolytic effect in response to HIF-1α, preferentially in cancer cells. The E1A partial deletion worked as an additional level of replication control. It contributed to the attenuation of the virus in normal cells without reducing the potency of the virus in cancer cells. The use of two broad-spectrum cancer-related promoters controlling these regions allows the dual control of the virus. In addition, having different sequences in both ends of the viral genome instead of duplicated promoters may contribute to the genetic stability of the virus. An important improvement of the new CRAds described here is the introduction of reporter/therapeutic genes in their genome. With Ad-DHLuc the kinetics of luciferase expression *in vivo* indicate an important amplification of the virus for a limited period. When using IL-12 as therapeutic gene, the transient but high level of transgene expression in the tumors may be sufficient to stimulate strong immune responses against cancer cells. In our group, we have used a NR-Ad vector encoding IL-12 to treat patients with pancreatic cancer metastatic to the liver.[27] The lack of clinically relevant responses in this trial was attributed in part to the low production of IL-12. Here, we provide evidence that Ad-DHscIL12 achieves much higher expression of IL-12 in pancreatic tumors, compared with a standard NR-Ad vector. In addition, replication-competent adenoviruses kills tumor cells, thus releasing tumor antigens that together with high IL-12 levels may promote efficient antitumor immunity and enhanced therapeutic effect. Moreover, the replication-competent adenovirus allows tumor-specific transgene expression, which was well tolerated in hamsters at therapeutic doses. Our main conclusion is that a replication-competent adenoviral vector can be used to obtain strong intratumor expression of IL-12 without increasing the toxicity of previously described vectors. However, further refinement of the system is desirable to increase the therapeutic index. Additional mechanisms that limit the systemic exposure to IL-12 could allow the use of higher doses of replication-competent vectors and favor the display of their oncolytic potential. In our model, the maximum tolerated dose for the intratumoral route of injection was 4×10^7 iu for Ad-DHscIL12; maximum tolerated dose for Ad-DHLuc was not reached at 2×10^9 iu; and maximum tolerated dose for wild-type adenovirus type 5 was not reached at 6×10^{10} iu in a similar model.[28] This clearly indicates that IL-12 expression, and not viral replication, determines the toxicity of Ad-DHscIL12.

The improvement of CRAds has been traditionally hampered by the lack of immunocompetent animal models in which replication of adenovirus takes place with a relevant efficiency. The need of such models is particularly evident if the therapeutic gene being delivered is an immunostimulatory cytokine. To our knowledge, there is only one previous study in which the antitumor effect of a CRAd expressing a cytokine (IFN-α) was evaluated in a Syrian hamster model of renal cancer.[29] High doses of the virus were repeatedly administered (up to 10 inoculations of 5×10^9 iu) to a subcutaneous tumor. The authors observed that the antitumor effect was enhanced by the expression of IFN-α, but an empty CRAd also showed tumor reduction. Here, we have used a model based on the intrahepatic dissemination of pancreatic cancer in which a single intratumor administration of Ad-DHscIL12 at a low dose (2×10^7 iu) halted progression of the disease in the majority the animals treated, and

achieved complete eradication in approximately half of them. In contrast, the same dose of Ad-DHLuc had no significant effect and also a higher dose (100-fold) of Ad-WTLuc (a nonrestricted adenovirus expressing luciferase) was unable to inhibit tumor growth. The poor responses observed with these last vectors recapitulate the results obtained in many clinical trials using CRAds, indicating that the oncolytic effect of adenovirus by itself is not sufficient to eradicate advanced tumors. This observation, together with the relatively low dose used in our experiments, implies that cancer cells that were not infected with the virus are being eliminated, raising the possibility of a systemic antitumor effect. In summary, we describe here that the expression of IL-12 in the context of a CRAd is efficient against pancreatic cancer in a relevant animal model. This approach can be readily tested in the clinical setting.

MATERIALS AND METHODS

Cell lines and culture. The human cell lines HEK 293 (ATCC#CRL-1573), A549 (lung cancer, ATCC# CCL-185), HuH-7 (hepatocellular carcinoma, courtesy of Dr Brechot, INSERM, Paris, France), BxPC-3 (pancreatic cancer ATCC#CRL-1687), PANC-1 (pancreatic cancer ATCC#CRL-1469), AsPC-1 (pancreatic cancer ATCC#CRL-1680), RCC10 and VHL53 (clear cell renal carcinoma, kindly provided by Dr del Peso, CSIC-UAM, Madrid, Spain), and the Syrian hamster pancreatic cancer cell line H2T[30] (courtesy of Dr Townsend, University of Texas Medical Branch, Galveston, TX), were maintained in DMEM supplemented with 10% fetal bovine serum (FBS). The NP18 cells (human pancreatic cancer,[31] courtesy of Dr Fillat, CRG, Barcelona, Spain) were maintained in RPMI supplemented with 10% FBS. The normal human fibroblasts IMR90 (ATCC#CCL-186) were cultured in MEM supplemented with 10% FBS, 1 mmol/l sodium pyruvate, and 0/1 mmol/l nonessential amino acids. All culture media were supplemented with 100 U/ml penicillin, 100 µg/ml streptomycin, and 2 mmol/l L-glutamine. All cells were maintained at 37 °C with 5% CO_2 in a humidified incubator. Hypoxia was induced by placing cells in hypoxic chambers (Billups Rothenberg, Del Mar, CA) with a mixture of gases containing 94% N_2, 6% CO_2, and 1% O_2.

Virus construction. The plasmid pSEHE2F has been previously described.[6] It contains the adenovirus type 5 genome with unique restriction sites flanking the E1A and E4 promoter regions that were substituted by tumor-specific promoters. We maintained the human E2F-1 core promoter in the E4 region and introduced the 9XHRE promoter in the E1A region, using BstBI sites. Using standard subcloning techniques the region comprising E3-6.7K/gp19K (bp 28,555–29,355 in the wild-type sequence) was deleted and flanked further by two ClaI sites. In this region, we introduced the firefly luciferase gene from the pGL3-Basic (Promega, Madison, WI). Starting from this plasmid (pSHE2F-Luc), a partial deletion was introduced into the E1A gene, comprising bp 922–947, to give rise to pSdlE2F-Luc. The murine scIL-12 gene[32] was obtained by PCR from the pSFG-mIL-12 plasmid (kindly provided by Dr Mulligan, Harvard Medical School, Boston, MA) and introduced into the ClaI sites of pSdlE2F-Luc using NarI restriction sites, to give rise to the pSDH-IL12 plasmid. The pAd-Luc plasmid was obtained by introducing the 12.5 kb fragment comprised between NdeI sites of the pSHE2F-Luc plasmid (containing the luciferase gene in the E3 region) into the pTG3602 plasmid,[33] thus restoring the wild-type structure of E1A and E4 regions. The recombinant viruses Ad-HLuc, Ad-DHLuc, Ad-DHscIL12, and Ad-WTLuc were generated after Calcium Phosphate transfection of the pSHE2F-Luc, pSdlE2F-Luc, pSDH-IL12, and pAd-Luc plasmids into 293 cells, respectively. The Ad-CMV-Luc virus was purchased from Vector Biolabs (Philadelphia, PA). The Ad-CMV-scIL12 is a standard NR-Ad carrying the scIL-12 under the control of a CMV promoter. It was constructed using the Adeno-X Expression System (Clontech, Mountain View, CA). All viruses were amplified in 293 cells and purified by ultracentrifugation in CsCl gradient. Quantification of infectious units (iu) was done using the Adeno-X rapid titer kit (Clontech).

Animals and treatment procedures. Tumor xenografts were induced in the flank of 5–6 weeks-old athymic *nu/nu* mice (Charles River Laboratories, Barcelona, Spain) by subcutaneous inoculation of 10^7 HuH-7 or H2T cells. When tumors reached a volume of 500–700 mm^3, viruses were injected intratumorally resuspended in 50 µl saline solution. Tumor volumes were calculated using the formula $V = (D \times d^2)/2$, where D and d are the major and minor diameters, respectively. Liver metastases of pancreatic cancer were established in Syrian (Golden) hamsters (*Mesocricetus Auratus*; *HSD HAN: AURA*, 5 weeks of age; Harlan, Barcelona, Spain) by intrahepatic injection of 2.5×10^6 H2T cells through laparotomy, as previously described.[25] Four to five weeks later, a single dose of each virus was injected intratumorally. Animals were sacrificed 30–35 days later and tumor volume measured as described above. All procedures were carried out following protocols approved by the local ethical committee in accordance with recommendations for proper care and use of laboratory animals.

In vivo *bioluminescence detection.* Ten minutes before luciferase detection, mice and hamsters received an intraperitoneal injection of 100 or 300 µl D-Luciferin Firefly (Xenogen, Alameda, CA), respectively. Animals were anesthetized and placed in a dark chamber connected to a cooled charge-coupled device camera (IVIS; Xenogen). Photon emission was quantified and analyzed using Living Image Software (Xenogen).

Micro-CT analysis. Hepatic contrast agent fenestra-LC (ART) was administered to hamsters at 10 ml/kg by retro-orbital injection. Ninety minutes later, animals were anesthetized and abdominal CT scan was performed using a Siemens MicroCAT-II scanner.

Western blotting. HIF-1α and fiber detection was performed in cell lysates, basically as previously described.[5,25] For fiber detection, cells were harvested in TNE buffer (50 mmol/l Tris pH 7.5, 5 mmol/l EDTA, 100 mmol/l NaCl) supplemented with 1% Igepal and a cocktail of protease inhibitors (Complete Tablets; Roche, Mannheim, Germany). After sonication, 10 µg of protein were separated on a 12% sodium dodecyl sulfate–polyacrylamide gel electrophoresis gel and transferred to a polyvinylidene difluoride membrane (Amersham Bioscience, Buckinghamshire, UK). Immunoblots were processed using 1: 10,000 dilution of primary monoclonal antibodies against fiber (Lab Vision, Fremont, CA), and 1:5,000 dilution peroxidase–conjugated goat antimouse IgG (Pierce, Rockford, IL). Detection was performed by Western Lighting chemiluminescence reagent (Perkin Elmer Life Sciences, Boston, MA). For HIF-1α detection cells were lyzed with RIPA buffer (65 mmol/l Tris pH 7.4; 150 mmol/l KCl; 1% Igepal; 0.1% sodium dodecyl sulfate) supplemented with protease inhibitors. Fifty µg of protein were separated on a 8% sodium dodecyl sulfate–polyacrylamide gel electrophoresis gel, transferred to nitrocellulose membrane (Whatman, Scleicher, and Schuell) and incubated with 1:1,000 primary antibody against HIF-1 α (BD Transduction Laboratories, San Jose, CA) and 1:5,000 peroxidase-conjugated goat antimouse IgG (Pierce). Immunolabeling was detected by Western Lighting chemiluminescence plus reagent (Perkin Elmer Life Sciences). Homogeneous sample loading was verified with an anti-glyceraldehyde-3-phosphate dehydrogenase antibody (AbD Serotec, Oxford, UK) at 1:5,000 dilution.

In vitro *viral replication assay (virus burst size).* Cells were infected at 10 and 100 iu/cell for cancer and normal cells, respectively. Viruses were removed 2 hours later, and cells were washed twice with PBS and incubated in DMEM supplemented with 2% FBS for 48 hours. Then cells were lyzed by three cycles of freezing and thawing and viruses were quantified by the Adeno X Rapid titer kit (BD Bioscience, San Diego, CA).

***Quantification of virus production* in vivo.** Tumors were frozen in liquid Nitrogen and 100–400 mg of tissue was homogenized in 1 ml of complete HEK293 growth medium. After three cycles of freezing and thawing, samples were centrifuged at 10,000*g* for 5 minutes and viruses in the supernatant were quantified by the Adeno X Rapid titer kit (BD Bioscience).

In vitro *viability assays.* Cells were seeded in 96-well tissue culture plates at 5×10^3 cells/well and 48 hours later they were infected with serial dilution of viruses. Cell viability was determined 5 or 7 days after infection by crystal violet staining. The percentage of survival is calculated by comparison with uninfected cells maintained in the same conditions (normoxia or hypoxia) as the infected cells. Data were analyzed using the PrismGraphPad program.

Immunohistochemistry. Tumor samples were embedded in Tissue Tek O.C.T (Sakura, Torrance, CA). Cryostat sections (5–7 μm) were air-dried and fixed in prechilled acetone for 10 minutes. Endogenous peroxidase was inhibited by incubation for 10 minutes at RT with Peroxidase Blocking Reagent (DakoCytomation, Carpinteria, CA). Tissue sections were incubated overnight at 4 °C with mouse antiadenovirus monoclonal antibody blend (Chemicon International, Temecula, CA) diluted 1:1,000. Then samples were incubated with 1:2,000 dilution of a goat antimouse antibody conjugated with horseradish peroxidase (Pierce). Sections were incubated for 5–10 minutes with a DAB substrate and finally counterstained with hematoxylin and mounted.

Quantification of murine IL-12 in serum. An OptEIA Mouse IL-12 ELISA kit was used (BD Biosciences) according to the manufacturer's instructions.

Quantitative reverse transcriptase-PCR. Analysis of hamster IFN-γ expression was performed as previously described.[34]

Determination of tumor-specific lymphocyte proliferation. Peripheral blood mononuclear cells from treated hamsters obtained 20 days after vector inoculation were exposed to tumor cells at 10:1 ratio and analyzed by flow cytometry 3 days after carboxyfluorescein succinimidyl ester labeling, basically as described in ref. 35. Data were analyzed using FlowJo software, and proliferation index was calculated.

Statistical analysis. The Mann–Whitney test was applied for statistical comparisons. Differences in survival curves were evaluated using the log-rank test. Analysis was performed using the GraphPad Prism program (GraphPad Software, San Diego, CA).

ACKNOWLEDGMENTS

We thank R.C. Mulligan (Department of Genetic, Harvard Medical School, Boston, MA) for the pSFG-mIL-12 plasmid, C.M. Townsend (University of Texas Medical Branch, Galveston, TX) for the H2T cells, C. Fillat (CRG, Barcelona, Spain) for the NP18 cells, L. del Peso (CSIC-UAM, Madrid, Spain) for renal carcinoma cell lines, and J.L. Romero-Trevejo (Morphology and Imaging Unit, Center for Applied Medical Research (CIMA), University of Navarra, Pamplona, Spain) for histological analysis. This project was founded through Grant SAF2003-08385 and SAF2006-04755 from the Spanish Department of Education and Science and the UTE project CIMA. R.H.A. is a recipient of a Ramon y Cajal Research Contract and IO is a recipient of a FPU fellowship from the Spanish Department of Education and Science. Funded in part by Instituto de Salud Carlos III. No conflict of interest from any of the authors exists.

REFERENCES

1. Aghi, M and Martuza, RL (2005). Oncolytic viral therapies—the clinical experience. *Oncogene* **24**: 7802–7816.
2. Rein, DT, Breidenbach, M and Curiel, DT (2006). Current developments in adenovirus-based cancer gene therapy. *Future Oncol* **2**: 137–143.
3. Le, QT, Denko, NC and Giaccia, AJ (2004). Hypoxic gene expression and metastasis. *Cancer Metastasis Rev* **23**: 293–310.
4. Chi, JT, Wang, Z, Nuyten, DS, Rodriguez, EH, Schaner, ME, Salim, A *et al.* (2006). Gene expression programs in response to hypoxia: cell type specificity and prognostic significance in human cancers. *PLoS Med* **3**: e47.
5. Cuevas, Y, Hernandez-Alcoceba, R, Aragones, J, Naranjo-Suarez, S, Castellanos, MC, Esteban, MA *et al.* (2003). Specific oncolytic effect of a new hypoxia-inducible factor-dependent replicative adenovirus on von Hippel-Lindau-defective renal cell carcinomas. *Cancer Res* **63**: 6877–6884.
6. Hernandez-Alcoceba, R, Pihalja, M, Qian, D and Clarke, MF (2002). New oncolytic adenoviruses with hypoxia- and estrogen receptor-regulated replication. *Hum Gene Ther* **13**: 1737–1750.
7. Cho, WK, Seong, YR, Lee, YH, Kim, MJ, Hwang, KS, Yoo, J *et al.* (2004). Oncolytic effects of adenovirus mutant capable of replicating in hypoxic and normoxic regions of solid tumor. *Mol Ther* **10**: 938–949.
8. Ide, T, Kitajima, Y, Miyoshi, A, Ohtsuka, T, Mitsuno, M, Ohtaka, K *et al.* (2007). The hypoxic environment in tumor-stromal cells accelerates pancreatic cancer progression via the activation of paracrine hepatocyte growth factor/c-Met signaling. *Ann Surg Oncol* **14**: 2600–2607.
9. Ide, T, Kitajima, Y, Miyoshi, A, Ohtsuka, T, Mitsuno, M, Ohtaka, K *et al.* (2006). Tumor-stromal cell interaction under hypoxia increases the invasiveness of pancreatic cancer cells through the hepatocyte growth factor/c-Met pathway. *Int J Cancer* **119**: 2750–2759.
10. Chen, L, Uchida, K, Endler, A and Shibasaki, F (2007). Mammalian tumor suppressor Int6 specifically targets hypoxia inducible factor 2 alpha for degradation by hypoxia- and pVHL-independent regulation. *J Biol Chem* **282**: 12707–12716.
11. Shen, BH and Hermiston, TW (2005). Effect of hypoxia on Ad5 infection, transgene expression and replication. *Gene Ther* **12**: 902–910.
12. Hahn, WC and Weinberg, RA (2002). Modelling the molecular circuitry of cancer. *Nat Rev Cancer* **2**: 331–341.
13. Johnson, DG, Ohtani, K and Nevins, JR (1994). Autoregulatory control of E2F1 expression in response to positive and negative regulators of cell cycle progression. *Genes Dev* **8**: 1514–1525.
14. Li, Y, Idamakanti, N, Arroyo, T, Thorne, S, Reid, T, Nichols, S *et al.* (2005). Dual promoter-controlled oncolytic adenovirus CG5757 has strong tumor selectivity and significant antitumor efficacy in preclinical models. *Clin Cancer Res* **11**: 8845–8855.
15. Jakubczak, JL, Ryan, P, Gorziglia, M, Clarke, L, Hawkins, LK, Hay, C *et al.* (2003). An oncolytic adenovirus selective for retinoblastoma tumor suppressor protein pathway-defective tumors: dependence on E1A, the E2F-1 promoter, and viral replication for selectivity and efficacy. *Cancer Res* **63**: 1490–1499.
16. Heise, C, Hermiston, T, Johnson, L, Brooks, G, Sampson-Johannes, A, Williams, A *et al.* (2000). An adenovirus E1A mutant that demonstrates potent and selective systemic anti-tumoral efficacy. *Nat Med* **6**: 1134–1139.
17. Fueyo, J, Gomez-Manzano, C, Alemany, R, Lee, PS, McDonnell, TJ, Mitlianga, P *et al.* (2000). A mutant oncolytic adenovirus targeting the Rb pathway produces anti-glioma effect *in vivo*. *Oncogene* **19**: 2–12.
18. Johnson, L, Shen, A, Boyle, L, Kunich, J, Pandey, K, Lemmon, M *et al.* (2002). Selectively replicating adenoviruses targeting deregulated E2F activity are potent, systemic antitumor agents. *Cancer Cell* **1**: 325–337.
19. Alonso, MM, Cascallo, M, Gomez-Manzano, C, Jiang, H, Bekele, BN, Perez-Gimenez, A *et al.* (2007). ICOVIR-5 shows E2F1 addiction and potent antiglioma effect *in vivo*. *Cancer Res* **67**: 8255–8263.
20. Del Vecchio, M, Bajetta, E, Canova, S, Lotze, MT, Wesa, A, Parmiani, G *et al.* (2007). Interleukin-12: biological properties and clinical application. *Clin Cancer Res* **13**: 4677–4685.
21. Bramson, JL, Hitt, M, Addison, CL, Muller, WJ, Gauldie, J and Graham, FL (1996). Direct intratumoral injection of an adenovirus expressing interleukin-12 induces regression and long-lasting immunity that is associated with highly localized expression of interleukin-12. *Hum Gene Ther* **7**: 1995–2002.
22. Caruso, M, Pham-Nguyen, K, Kwong, YL, Xu, B, Kosai, KI, Finegold, M *et al.* (1996). Adenovirus-mediated interleukin-12 gene therapy for metastatic colon carcinoma. *Proc Natl Acad Sci USA* **93**: 11302–11306.
23. Putzer, BM, Hitt, M, Muller, WJ, Emtage, P, Gauldie, J and Graham, FL (1997). Interleukin 12 and B7-1 costimulatory molecule expressed by an adenovirus vector act synergistically to facilitate tumor regression. *Proc Natl Acad Sci USA* **94**: 10889–10894.
24. Thomas, MA, Spencer, JF, La Regina, MC, Dhar, D, Tollefson, AE, Toth, K *et al.* (2006). Syrian hamster as a permissive immunocompetent animal model for the study of oncolytic adenovirus vectors. *Cancer Res* **66**: 1270–1276.
25. Bortolanza, S, Alzuguren, P, Bunuales, M, Qian, C, Prieto, J and Hernandez-Alcoceba, R (2007). Human adenovirus replicates in immunocompetent models of pancreatic cancer in Syrian hamsters. *Hum Gene Ther* **18**: 681–690.
26. Hawkins, LK, Johnson, L, Bauzon, M, Nye, JA, Castro, D, Kitzes, GA *et al.* (2001). Gene delivery from the E3 region of replicating human adenovirus: evaluation of the 6.7 K/gp19 K region. *Gene Ther* **8**: 1123–1131.
27. Sangro, B, Mazzolini, G, Ruiz, J, Herraiz, M, Quiroga, J, Herrero, I *et al.* (2004). Phase I trial of intratumoral injection of an adenovirus encoding interleukin-12 for advanced digestive tumors. *J Clin Oncol* **22**: 1389–1397.
28. Thomas, MA, Spencer, JF, Toth, K, Sagartz, JE, Phillips, NJ and Wold, WS (2008). Immunosuppression enhances oncolytic adenovirus replication and antitumor efficacy in the Syrian hamster model. *Mol Ther* **16**: 1665–1673.
29. Shashkova, EV, Spencer, JF, Wold, WS and Doronin, K (2007). Targeting Interferon-alpha Increases Antitumor Efficacy and Reduces Hepatotoxicity of E1A-mutated Spread-enhanced Oncolytic Adenovirus. *Mol Ther* **15**: 598–607.
30. Townsend, CM Jr, Franklin, RB, Gelder, FB, Glass, E and Thompson, JC (1982). Development of a transplantable model of pancreatic duct adenocarcinoma. *Surgery* **92**: 72–78.
31. Reyes, G, Villanueva, A, Garcia, C, Sancho, FJ, Piulats, J, Lluis, F *et al.* (1996). Orthotopic xenografts of human pancreatic carcinomas acquire genetic aberrations during dissemination in nude mice. *Cancer Res* **56**: 5713–5719.
32. Lieschke, GJ, Rao, PK, Gately, MK and Mulligan, RC (1997). Bioactive murine and human interleukin-12 fusion proteins which retain antitumor activity *in vivo*. *Nat Biotechnol* **15**: 35–40.
33. Chartier, C, Degryse, E, Gantzer, M, Dieterle, A, Pavirani, A and Mehtali, M (1996). Efficient generation of recombinant adenovirus vectors by homologous recombination in Escherichia coli. *J Virol* **70**: 4805–4810.
34. Rama Iniguez, S, Dea-Ayuela, MA, Sanchez-Brunete, JA, Torrado, JJ, Alunda, JM and Bolas-Fernandez, F (2006). Real-time reverse transcription-PCR quantification of cytokine mRNA expression in golden Syrian hamster infected with Leishmania infantum and treated with a new amphotericin B formulation. *Antimicrob Agents Chemother* **50**: 1195–1201.
35. Gujar, SA and Michalak, TI (2005). Flow cytometric quantification of T cell proliferation and division kinetics in woodchuck model of hepatitis B. *Immunol Invest* **34**: 215–236.